

Self-consistent kinetic theory of a plasma sheath

Aleksey V. Vasenkov* and Bernie D. Shizgal†

Department of Chemistry, University of British Columbia, 2036 Main Mall, Vancouver, British Columbia, Canada V6T 1Z1

(Received 26 June 2001; published 25 March 2002)

A fully kinetic theory model of the sheath of a dc glow discharge is presented. This model includes a direct numerical solution of Boltzmann equations for the spatial and velocity dependence of the electron and Ar^+ distribution functions with a self-consistent electric field calculated from the Poisson equation. The solution is obtained using a collocation method that employs Legendre quadrature points for both angular and spatial variables, and nonclassical speed quadrature points for velocity. The results of the steady state direct numerical solution are compared with a particle-in-cell Monte Carlo simulation. As anticipated, it is found that the space- and energy-dependent ion distribution function varies strongly with a decrease in the ratio of the Debye length to the ion mean free path.

DOI: 10.1103/PhysRevE.65.046404

PACS number(s): 52.40.Hf, 52.65.Rr, 52.25.Dg, 52.80.-s

I. INTRODUCTION

In the study of electron and ion transport in discharge devices, an important consideration is the nonequilibrium behavior of ions and electrons close to an electrode. This region is referred to as the sheath, and is not rigorously defined. The motion of electrons in the sheath region is strongly coupled with that of ions. The plasma sheath potential is not known *a priori* but must be found self-consistently. Understanding the basic properties of plasma sheath is a significant problem in discharge physics, plasma chemistry, gaseous laser physics, and especially in plasma processing. In this paper, we treat an idealized system consisting of a collection of Ar^+ , Ar, and e^- , bounded at the spatial origin ($r=0$) by an absorbing electrode. The physical situation is depicted in Fig. 1 of [1]. In addition, fluxes of electron and ions are specified at $r \rightarrow 0$, and there is no ionization considered.

Far from the electrode in the bulk plasma, a macroscopic fluid description based on the differential fluid dynamic equations for the fluid variables such as the density, flow velocity, and temperature is valid. This fluid description can be derived from the kinetic description, and is a simpler approach in that there is a reduction in the dimensionality of the variables involved. Close to the surface, the hydrodynamic approach is no longer valid and a *microscopic* description based on kinetic theory that involves a determination of the system distribution functions from the Boltzmann equation must be used. An understanding of nonequilibrium phenomena in plasma sheaths is a fundamental problem. The problem overlaps many other problems in science and engineering, which include boundary layers that occur in laser physics, fusion devices, aeronautics, space science, astrophysics, chemically reactive systems, radiation physics, etc. This paper addresses a fundamental problem involving the development of kinetic theory methods for the description of

plasma sheaths and the assessment of the validity of fluid dynamic models.

The study of plasma sheaths has a very long history. The first important studies are the classic works by Tonks and Langmuir [2] and by Self [3,4]. Recent papers [5–9] have provided brief historical accounts of the previous theoretical work. Recent (analytic) models have been presented by Riley [10,11], by Metze *et al.* [12], and by Lieberman [13]. Riemann [14,15] has given a very detailed and comprehensive review of sheath formation and the Bohm criterion. The generalized Bohm criterion is used as a boundary condition at the plasma-sheath interface. Sheridan and Goree [16] have studied the effects of collisionality on the plasma sheath with a two-fluid model. Procassini *et al.* [8] have considered a particle-in-cell (PIC) model of a collisionless plasma that contacts a floating absorbing boundary. They studied the effect of different source distributions and their model does not involve the usual assumption of the Boltzmann relation for electrons. Scheuer and Emmert [9] reported on a kinetic approach based on the Boltzmann equation but with a simple Bhatnagar-Gross-Krook (BGK) model of the collision operator. This is a poor model for ion-ion collisions for which a Fokker-Planck collision term should be used. Koch and Hitchon [17] considered a computer simulation of the effects of collisions on the plasma presheath with a Green's function approach. They studied the effect of charge exchange collisions and different source functions as did Scheuer and Emmert [9]. Hong and Emmert [18] employed a two-dimensional fluid theory for cold collisionless ions coupled to the Poisson equation. They considered time dependent sheaths, which has important applications to plasma source ion implantation process. Van den Berg *et al.* [7] considered a collisionless Boltzmann equation with a source term. Their main objective was to study the Bohm criterion and the sheath edge field singularity. The choice of source term is made to permit an analytical evaluation of the results.

Valentini and co-workers [19,20] have applied a two-fluid model to a positive column in cylindrical geometry. They emphasized the importance of properly treating boundary sheaths for several technical applications. In particular, they mention that a proper understanding of sheath phenomena requires a kinetic theory treatment but they employ a hydro-

*Mailing address: Institute of Thermophysics, Novosibirsk, 630090, Russia. Email address: vasenkov@theory.chem.ubc.ca

†Email address: shizgal@theory.chem.ubc.ca; URL: <http://www.chem.ubc.ca/personnel/faculty/shizgal/>

dynamic approach. They use multiscale theories and special matching conditions together with the Bohm criterion to determine the sheath edge. Nitschke and Graves [21] have also considered a matching of a sheath model with a fluid bulk plasma model. They mention that fully resolving the sheath can be computationally expensive due to the different length scales of the sheath and the bulk plasma. They emphasize the arbitrariness of these matching procedures. Godyak and Sternberg [22,23] again emphasize that there is an urgent need to consider the sheath and the bulk plasma together as one system. Dalvie *et al.* [24] reported Monte Carlo (MC) simulations with a self-consistent electric field obtained from the solution of the Poisson equation. These authors performed MC simulations with the use of constant collision cross sections. The use of this unrealistic collisional model allows for a very simple MC algorithm. The present work employs realistic cross sections in a fully kinetic theory treatment coupled to the Poisson equation, whereas many of the previous models are fully or partially based on hydrodynamics.

In Sec. II, we present our kinetic model of the sheath. The direct numerical solution (DNS) of the Boltzmann equations for electron and ion distribution functions with a self-consistent electric field obtained from the Poisson equation is described in detail. A brief summary of our PIC-MC method is also presented in this section. In Sec. III, the results of calculations are presented for the sheath region in a DC glow discharge in Ar.

II. SELF-CONSISTENT KINETIC THEORY OF A PLASMA SHEATH

A. Direct numerical solution

The self-consistent model of electron and ion transport in a boundary layer between the plasma and an electrode requires the solution of the Boltzmann equations for the distribution functions of electrons, $\tilde{f}_e(r, \mathbf{v}, t)$, and ions $\tilde{f}_i(r, \mathbf{v}, t)$, and is coupled to the Poisson equation for the self-consistent field. We consider a one-dimensional discharge such that the spatial dependence is only in the r axis. We consider a system of electrons and ions dilutely dispersed in background of atoms considered at equilibrium. The Boltzmann equations for the electron and ion distribution functions are given by

$$\frac{\partial \tilde{f}_e}{\partial t} + \mu v \frac{\partial \tilde{f}_e}{\partial r} - \mu \frac{e\tilde{E}}{m_e} \frac{\partial \tilde{f}_e}{\partial v} = n_g \tilde{J}_e[\tilde{f}_e], \quad (1)$$

$$\frac{\partial \tilde{f}_i}{\partial t} + \mu v \frac{\partial \tilde{f}_i}{\partial r} + \mu \frac{e\tilde{E}}{M_i} \frac{\partial \tilde{f}_i}{\partial v} = n_g \tilde{J}_i[\tilde{f}_i], \quad (2)$$

where $\mu = \cos \theta$, and θ is the angle relative to the r axis; m_e and M_i are the electron and ion masses, respectively; and n_g is the neutral gas density. We have written the time-dependent forms of the Boltzmann equations, although it is the steady distributions that are desired. The electric field, E , in Eq. (1) is determined from the Poisson equation,

$$\frac{\partial \tilde{E}}{\partial r} = \frac{e}{\epsilon_0} (\tilde{n}_i - \tilde{n}_e), \quad (3)$$

where e is the electron charge and ϵ_0 is the vacuum permittivity. The electric field is derivable from the scalar potential, φ , that is,

$$\tilde{E} = - \frac{\partial \tilde{\varphi}}{\partial r}, \quad (4)$$

where the steady electron and ion densities, $n_e(r)$ and ions $n_i(r)$, respectively, are determined by

$$\tilde{n}_e(r) = \int \tilde{f}_e(r, v, \mu) dv, \quad (5)$$

$$\tilde{n}_i(r) = \int \tilde{f}_i(r, v, \mu) dv. \quad (6)$$

We have suppressed the time variable as it is the steady distribution functions sought. The linear collision operator for electron-neutral interactions, \tilde{J}_e , is given by the Lorentz-Fokker-Planck form [25,26]

$$\begin{aligned} \tilde{J}_e[\tilde{f}] = & \frac{m_e}{M} \frac{1}{v^2} \frac{\partial}{\partial v} \left\{ \left[\sigma_m(v) v^4 \left(1 + \frac{kT_1}{m_e v} \frac{\partial}{\partial v} \right) \right] \tilde{f}_e(r, v, \mu) \right\} \\ & + \frac{\sigma_m(v) v}{2} \frac{\partial}{\partial \mu} \left\{ (1 - \mu^2) \frac{\partial}{\partial \mu} [\tilde{f}_e(r, v, \mu)] \right\}, \quad (7) \end{aligned}$$

where $\sigma_m(v)$ is the momentum transfer cross section, M and T_1 are the atom mass and the temperature of background medium, respectively. The first term in curly brackets in Eq. (7) is the isotropic portion of the operator whereas the second term is the anisotropic part that describes pitch-angle scattering.

We assume that the major process for ion-neutral collision is the charge exchange process for which the collision operator, \tilde{J}_i , is of the form

$$\begin{aligned} \tilde{J}_i[\tilde{f}_i(r, v, \mu)] = & \tilde{f}_i^M(v) \int \tilde{f}_i(r, v', \mu) \sigma_{ex}(g) g d\mathbf{v}' \\ & - \tilde{f}_i(r, v, \mu) \int \tilde{f}_i^M(v') \sigma_{ex}(g) g d\mathbf{v}', \quad (8) \end{aligned}$$

where $\sigma_{ex}(v)$ is the charge exchange cross section, $g = |\mathbf{v} - \mathbf{v}'|$ is the relative velocity. In Eq. (8), the Maxwellian distribution is defined by, $\tilde{f}_i^M(v) = (M_i/2\pi kT_1)^{3/2} \exp(-M_i v^2/2kT_1)$. When written explicitly in terms of spherical velocity components, this operator for charge exchange collisions of ions with neutrals is given by

$$\begin{aligned}
 \tilde{J}_i[\tilde{f}_i] &= (M_i/2\pi kT_1)^{3/2} \exp(-M_i v^2/2kT_1) \\
 &\times \int_0^\infty \int_{-1}^1 \int_0^{2\pi} \sigma_{ex}(g) g \tilde{f}_i(r, v', \mu) \\
 &\times v'^2 dv' d\mu d\phi \\
 &- (M_i/2\pi kT_1)^{3/2} \tilde{f}_i(r, v, \mu) \int_0^\infty \int_{-1}^1 \int_0^{2\pi} \sigma_{ex}(g) g \\
 &\times \exp(-M_i v'^2/2kT_1) v'^2 dv' d\mu d\phi. \quad (9)
 \end{aligned}$$

We introduce the ion mean free path, $L_i = 1/n_g \sigma_i$ and the reference density given by $n_0 = j_0/D_a n_g \sigma_0$ with the flux $j_0 = 1 \text{ cm}^{-2} \text{ s}^{-1}$. Here $\sigma_0 = 1 \text{ \AA}$, D_a is the ambipolar diffusion coefficient, and σ_i is the charge exchange cross section calculated at energy corresponding to the ion temperature T_i chosen far from the electrode. We also introduce dimensionless spatial variable defined as $x = r/L_i$ and dimensionless velocity variables for electrons, $p = v/v_e$, and ions, $P = v/v_i$ where $v_e = (2kT_e/m_e)^{1/2}$ and $v_i = (2kT_i/M_i)^{1/2}$. Similarly, we define dimensionless times for electrons and ions, $t_e = \tilde{t}v_e/L_i$, $t_i = \tilde{t}v_i/L_i$, respectively. Although the definition of dimensionless variables is not unique and other definitions could be used, this definition is conventional. The distribution functions, densities, collision operators and fields can thus be written in dimensionless form and we have that, $f_e = \tilde{f}_e v_e^3/n_0$, $f_i = \tilde{f}_i v_i^3/n_0$, $n_e = \tilde{n}_e/n_0$, $n_i = \tilde{n}_i/n_0$, $J_e[f] = \tilde{J}_e[\tilde{f}]/(\sigma_i v_e)$, $J_i[f] = \tilde{J}_i[\tilde{f}]/(\sigma_i v_i)$, $E = e\tilde{E}L_i/kT_e$, $\varphi = e\tilde{\varphi}/kT_e$. With the transformation to these dimensionless variables, Eqs. (1)–(3) can be rewritten as the system of equations

$$\frac{\partial f_e}{\partial t_e} + \mu p \frac{\partial f_e}{\partial x} - \frac{\mu E}{2} \frac{\partial f_e}{\partial p} = J_e[f_e], \quad (10)$$

$$\frac{\partial f_i}{\partial t_i} + \mu P \frac{\partial f_i}{\partial x} + \frac{\mu E}{2} \frac{T_e}{T_i} \frac{\partial f_i}{\partial P} = J_i[f_i], \quad (11)$$

$$n_e(x) = \int f_e(p, x, \mu) d\mathbf{p}, \quad (12)$$

$$n_i(x) = \int f_i(P, x, \mu) d\mathbf{P}, \quad (13)$$

$$\frac{\partial E}{\partial x} = \varepsilon^{-2}(n_i - n_e), \quad (14)$$

$$E = -\frac{\partial \varphi}{\partial x}, \quad (15)$$

where $\varepsilon = \lambda_D/L_i$ and λ_D is the Debye length given by $\lambda_D = (\varepsilon_0 kT_e/n_0 e^2)^{1/2}$. The ratio of the electron temperature to ion temperature appears in Eq. (11) because T_i is used to

introduce the dimensionless ion velocity, whereas electric field is divided by T_e . The parameter ε controls the spatial variation of the electric field and indirectly, owing to the coupling of the Poisson equation with the Boltzmann equations, the other variables: distribution function, density, temperature, etc. As $\varepsilon \rightarrow 0$, the problem is then a two scale problem with variation of system properties on an L_i length scale as well as a λ_D length scale. In the extreme limit, asymptotic methods are used [15].

The steady distributions for both electrons and ions are determined from the time-dependent Eqs. (10) and (11), respectively. The time derivatives in Eqs. (10) and (11) are reduced to algebraic form with an explicit finite difference method, that is,

$$f_e^{n+1} = f_e^n - B_e \Delta t_e, \quad (16)$$

$$f_i^{n+1} = f_i^n - B_i \Delta t_i, \quad (17)$$

where $n+1$ and n denote successive times separated by Δt . The quantities B_e and B_i are evaluated at time denoted by n and are defined by,

$$B_e = p \mu \frac{\partial f_e}{\partial x} - \frac{\mu E}{2} \frac{\partial f_e}{\partial p} - J_e[f_e], \quad (18)$$

$$B_i = P \mu \frac{\partial f_i}{\partial x} + \frac{\mu E}{2} \frac{T_e}{T_i} \frac{\partial f_i}{\partial P} - J_i[f_i]. \quad (19)$$

Equations (18) and (19) are discretized with a collocation method that employs Legendre quadrature points for both the μ and x variables, and the nonclassical speed quadrature points for p and P . The derivative operators in x , p , and P in Eqs. (18) and (19) are replaced with their matrix representatives as discussed by Shizgal [27], and Blackmore and Shizgal [28]. The discretization is based on a discrete matrix derivative operator defined such that

$$\left. \frac{dF(x)}{dx} \right|_{x=x_i} = \sum_{j=1}^N D_{ij} F(x_j). \quad (20)$$

This algorithm permits the reduction to algebraic form of differential operators as occurs explicitly in Eqs. (18) and (19). The electron collision operator in the form of a differential Fokker-Planck operator in Eq. (8) can also be written in terms of first and second order derivative operators [26]. Equation (18) is thus written in discrete form as given by

$$\begin{aligned}
B_e(x_k, p_n, \mu_l) = & p_n \mu_l \sum_{j=1}^{N_x} D_{kj}^L f_e(x_j, p_n, \mu_l) \\
& - \frac{\mu_l E_k}{2} \sum_{j=1}^{N_p} D_{nj}^S f_e(x_k, p_j, \mu_l) \\
& - \frac{m_e}{M} \frac{1}{p_n^2} \sum_{j=1}^{N_p} D_{nj}^S \frac{\sigma_m(p_j)}{\sigma_i} p_j^4 \left[f_e(x_k, p_j, \mu_l) \right. \\
& \left. + \frac{1}{2p_j} \sum_{i=1}^{N_p} D_{ji}^S f_e(x_k, p_i, \mu_l) \right] \\
& - \frac{\sigma_m(p_n)}{2\sigma_i} \sum_{j=1}^{N_\mu} D_{ij}^L (1 - \mu_j^2) \\
& \times \sum_{i=1}^{N_\mu} D_{ji}^L f_e(x_k, p_n, \mu_i), \tag{21}
\end{aligned}$$

where D_{kj}^L and D_{nj}^S are the derivative matrix operators for Legendre and speed quadratures, respectively. The quantities, N_x , N_p , and N_μ are the number of discrete quadrature points in the x , p , and μ variables. The first two terms in Eq. (21) correspond to the derivative terms in Eq. (18). The third term involving the square brackets is the isotropic portion of the electron-atom collision operator whereas the last term involving the derivatives in μ arise from the anisotropic part of the collision operator. The ion-neutral charge exchange integral operator can be evaluated using the quadrature formula for the speed weight function [27,28]. The discrete form of Eq. (19) follows similarly except that the ion-neutral charge exchange collision operator is an integral operator and evaluated with the speed quadrature formula, that is,

$$\begin{aligned}
B_i(x_k, p_n, \mu_l) = & p_n \mu_l \sum_{j=1}^{N_x} D_{kj}^L f_i(x_j, p_n, \mu_l) \\
& + \frac{\mu_l E_k}{2} \frac{T_e}{T_i} \sum_{j=1}^{N_p} D_{nj}^S f_i(x_k, p_j, \mu_l) \\
& - \frac{2}{\pi^{3/2}} \exp(-P_n^2) \sum_{j=1}^{N_p} w_j^S \exp(P_j^2) \\
& \times \sum_{i=1}^{N_\mu} \sum_{m=1}^{N_\mu} w_i^L w_m^L \frac{V_{jnilm}}{(1 - \mu_m^2)} \frac{\sigma_{ex}(V)}{\sigma_i} \\
& \times f_i(x_k, p_j, \mu_i) + \frac{2}{\pi^{3/2}} f_i(x_k, p_n, \mu_l) \\
& \times \sum_{j=1}^{N_p} \sum_{i=1}^{N_\mu} \sum_{m=1}^{N_\mu} w_j^S w_i^L w_m^L \frac{V_{jnilm}}{(1 - \mu_m^2)} \frac{\sigma_{ex}(V)}{\sigma_i}, \tag{22}
\end{aligned}$$

where $V_{jnilm} = P_j^2 + P_n^2 - 2P_n P_j \mu_{ilm}$, $\mu_{ilm} = \mu_l \mu_i - [(1$

$-\mu_l^2)(1 - \mu_i^2)]^{1/2} \mu_m$. The electric field at the j th collocation position was found from a solution of the Poisson equation given by

$$E(x_j) = \sum_k D_{kj}^{-1} \varepsilon^{-2} [n_i(x_j) - n_e(x_j)]. \tag{23}$$

The electric field as $x \rightarrow \infty$ is calculated from the requirement that the motion of electrons and ions is described by the ambipolar diffusion [29],

$$E(x)|_{x \rightarrow \infty} = \frac{D_i - D_a}{D_i} \frac{1}{x},$$

where the ambipolar diffusion coefficient is given by [29]

$$D_a = \frac{D_e \mu_i + D_i \mu_e}{\mu_e + \mu_i}.$$

Here D_e, D_i , and μ_e, μ_i are the electron and ion coefficients of diffusion and mobility, respectively.

The method of solution follows earlier treatments of the Milne problem [1,26,28]. The distribution function, f_i^0 , and electron distribution function, f_e^0 , far from the boundary at $x=0$ given by

$$\begin{aligned}
f_e^0(x_k, p_n, \mu_l) = & f_i^0(x_k, p_n, \mu_l) \\
= & -j_0 / D_a f^M(p_n) [q_a + x_k - \mu_l U(p_n)] \tag{24}
\end{aligned}$$

serve as asymptotic boundary conditions. The coefficient q_a is the extrapolation length [1,26]. These distribution functions are the asymptotic forms consistent with the Chapman-Enskog type solution of the diffusion of ions or electrons through the background neutral gas at equilibrium. The distribution functions are close to Maxwellians with a small perturbation owing to the finite drift of electrons and ions. The perturbation is of the form [1]

$$\mu_l U(p_n) = \sum_{n=0}^N d_n \psi_{n1}(p_n, \mu_l),$$

where the basis functions $\psi_{ni}(p_n, \mu_l)$ are the Laguerre-spherical harmonic basis functions.

The extrapolation length q_a , and the expansion coefficients d_n (which describe ambipolar transport of electrons and ions far from the electrode) are calculated from the solution of the Boltzmann equation [1,26] with the collision operator I equal to

$$I = \frac{T_e}{T_e + T_i} \left(J_e[f] + \frac{T_i}{T_e} J_i[f] \right). \tag{25}$$

This choice for the collision operator I reduces the system of equations (10)–(15) to one equation. The temperature factors in Eq. (25) occur because T_i and T_e are used to introduce the dimensionless velocities in Boltzmann equations for ion and electron distribution functions, respectively.

The numerical solution of system of equations (16)–(23) is obtained as given by the iterations in Eqs. (16) and (17). The initial distribution functions for electrons and ions in this time-dependent approach to steady state are chosen according to the distribution represented by Eq. (24). The algorithm includes cycles, each of which involves the direct numerical solution of the Boltzmann equations for electron and ion distribution functions, subject to the Marshak boundary conditions [26], and the Poisson equation for the self-consistent electric field. The electron and ion distribution functions at the time t_n are given by Eqs. (18) and (19), respectively. The electric field, used in Eqs. (18) and (19), is calculated by solving Eq. (23) that employs the electron and ion densities obtained at t_{n-1} . This procedure is repeated until the steady state solution of Eqs. (18) and (19) is obtained.

B. The stochastic simulation

A PIC simulation is a widely used alternative approach to the direct solution of the system of equations (1)–(3). In the PIC method, a group of electrons (or ions) is represented by a single simulation particle. It is usually assumed that this particle has only short-range interactions with a gas atom that correspond to collisions. The statistical Monte Carlo collision technique is used to simulate these collisions. In the PIC-MC method, each particle moves in the electric field according to Newton's law. The self-consistent field is calculated from the solution of the Poisson equation with the density of electrons and ions obtained from the particle simulation.

In this study, we use the PIC-MC algorithm to study the steady space- and energy-dependent ion and electron distributions in the sheath region. The algorithm includes a Monte Carlo simulation of charged particle transport in a self-consistent electric field calculated using the Poisson equation. Ensembles of electrons and ions with Maxwellian speed distributions are incident on the gas medium of finite extent in the r direction. The Monte Carlo simulation of particle collisions, neglecting Coulomb collisions, with a velocity dependent collision cross section is made tractable by the null-collision technique. This is accomplished by adding an additional fictitious process referred to as null collisions such that the total collision frequency is constant at the value $\nu_m^l = n_g g [\sigma_{null}^l(g) + \sigma^l(g)]$, where l is either e for electrons or i for ions and g is the relative velocity. The real cross section is $\sigma^l(g)$ and $\nu(g) = n_g \sigma^l(g)$ is the total collision frequency for real collisions. This technique was developed by Skullerud [30] and discussed by others [31,32]. The probabilities of real and null collisions are then given by

$$P_{real}^l(g) = \nu(g) / \nu_m^l, \quad (26)$$

$$P_{null}^l(g) = [\nu_m^l - \nu(g)] / \nu_m^l. \quad (27)$$

The simulation domain is divided into cells, sufficiently small, so that there no appreciable change in the electric field within a cell. The trajectory of a charged particle in free flight in a cell is described with the Newton's equation of motion and energy conservation. With the null collision tech-

nique, the time between collisions, τ_l , is calculated with $\tau_l = -\ln(R) / \nu_m^l$, where R is a random number. In contrast to the usual PIC-MC simulation, we have that $\tau_e > \tau_i$, so that ions usually do not traverse more than one cell in time τ_i , while electrons often cross several cells in time τ_e . The trajectory of each particle is characterized by a succession of free flights interrupted by collisions. In the case of null collisions, a particle emerges with no change in velocity.

Electron-neutral collisions are treated with an isotropic momentum transfer cross section with no energy transfer occurring owing to the small electron mass. The approach used for ion-neutral charge exchange collisions involves sampling the velocity of the neutrals from a Maxwellian distribution. The probability of a charge exchange collision is then determined with Eq. (26). If an ion experiences a charge exchange collision then it is replaced by a newly created ion. The velocity of the new ion is determined by treating a charge-transfer collision as a head-on collision with a scattering angle of π .

The core of our algorithm consists of three primary procedures: the simulation of collisions, indexing, and cross referencing of particles, and the simulation of particle motion. At the end of third procedure, spatial distributions of electrons and ions are obtained using the spatial coordinates and velocity components of simulation particles,

$$n_s(r) = \frac{\sum_k n_s^k(r, \mathbf{p})}{\Delta r}, \quad (28)$$

where the subscript s represents the kind of particle (e for electrons and i for ions), $n_s^k(r, \mathbf{p})$ is the space- and velocity-dependent distribution function. The summation in Eq. (28) is over all particles in the spatial interval Δr centered at r . The Poisson equation is solved with the quadrature discretization method, which permits the reduction of the differential operator to the algebraic form. The details of solution are given in the preceding subsection. These procedures are repeated until the steady state distributions of ions and electrons are obtained.

The present model is used to determine the space and energy dependent ion and electron distribution functions,

$$f_s(r, E) = \frac{\sum_k n_s^k(r, \mathbf{p})}{\Delta r \Delta E}, \quad (29)$$

where the summation is over all particles existing in the spatial interval Δr centered at r , and also, in the energy interval ΔE centered at E .

III. RESULTS AND DISCUSSION

The main objective of this paper is to determine space- and velocity-dependent distribution functions of electrons and ions near an electrode. Both direct numerical solutions of Eqs. (16)–(23) and PIC-MC simulation were considered. The momentum transfer cross section for the electron-Ar elastic collisions was taken from Ref. [33], whereas the charge-exchange cross section for Ar^+ -Ar interactions was obtained using the results from Ref. [34]. The electron and

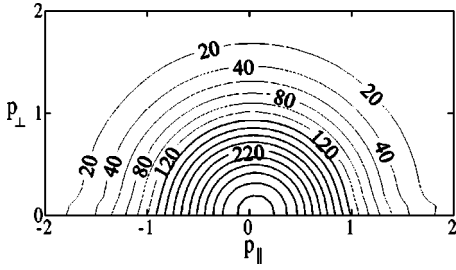


FIG. 1. Ion distribution function $f_i(x, P_\perp, P_\parallel)$ in units of $10^{-2}n_0/v_i^3$ is shown as a function of dimensionless perpendicular (P_\perp) and parallel (P_\parallel) velocities, $x=77.35$.

ion velocity distribution functions far from the electrode were chosen to be Maxwellian distributions for electrons and ions with $T_e=3000$ K and $T_i=300$ K. The background gas temperature was equal to 300 K.

The distribution function of ions (or electrons) far from the electrode, given by Eq. (24), is presented in Fig. 1. The distribution function, $f_i^0(x, p, \mu)$, denoted by $f_i(x, P_\perp, P_\parallel)$ is shown as function of dimensionless perpendicular, $P_\perp = P\sqrt{1-\mu^2}$, and parallel, $P_\parallel = P\mu$, velocities. We see that the distribution shown in Fig. 1 is slightly anisotropic. The position of the maximum is also slightly shifted from the origin due to the drift of ions towards to the electrode.

We obtain the steady ion and electron distribution functions, which are the primary objectives, by solving the time-dependent Boltzmann equations, Eqs. (16)–(19). The distribution functions in Eq. (24), shown in Fig. 1, are the same as the ion and electron initial distributions for the time-dependent calculations. The time evolution of the ion distribution, $f_i(x, P_\perp, P_\parallel, t)$, in the region close to the electrode, obtained using the direct numerical solution described in Sec. II, is shown in Figs. 2(A) and 2(B) for $x=0.124$ and $x=0.681$, respectively, at reduced times t_i equal to 0.08 (a), 0.23 (b), 0.77 (c). We see in Fig. 2(A) that the angular distribution of ions calculated at $t_i=0.08$ is rather anisotropic, and this distribution includes a few ions with negative P_\parallel . This is because of the absorbing boundary condition at the electrode used in the solution of the Boltzmann equation. The angular distributions, calculated at $t_i=0.23$ and $t_i=0.77$, show that degree of anisotropy decays with an increase in time, owing to ion-neutral charge exchange collisions. The time evolution of the ion angular distribution at $x=0.681$ is shown in Fig. 2(B). In this case, the angular distribution of ions relaxes to an almost isotropic steady distribution in c.

The steady distributions $f_i(x, P_\perp, P_\parallel)$ and $f_e(x, p_\perp, p_\parallel)$ calculated at different positions from the electrode, are compared in Figs. 3(A) and 3(B), respectively, at reduced distances x from the electrode equal to 0 (a), 0.124 (b), and 0.681 (c). The angular distribution of electrons is slightly more anisotropic than that for ions for $x=0$. The differences between the ion and electron angular distributions become considerable away from the electrode (b). The degree of anisotropy in both $f_i(x, P_\perp, P_\parallel)$ and $f_e(x, p_\perp, p_\parallel)$ decreases with an increase of distance. In the region close to the electrode, the anisotropy in $f_i(x, P_\perp, P_\parallel)$ decays because of charge-exchange collisions, while the degree of anisotropy in

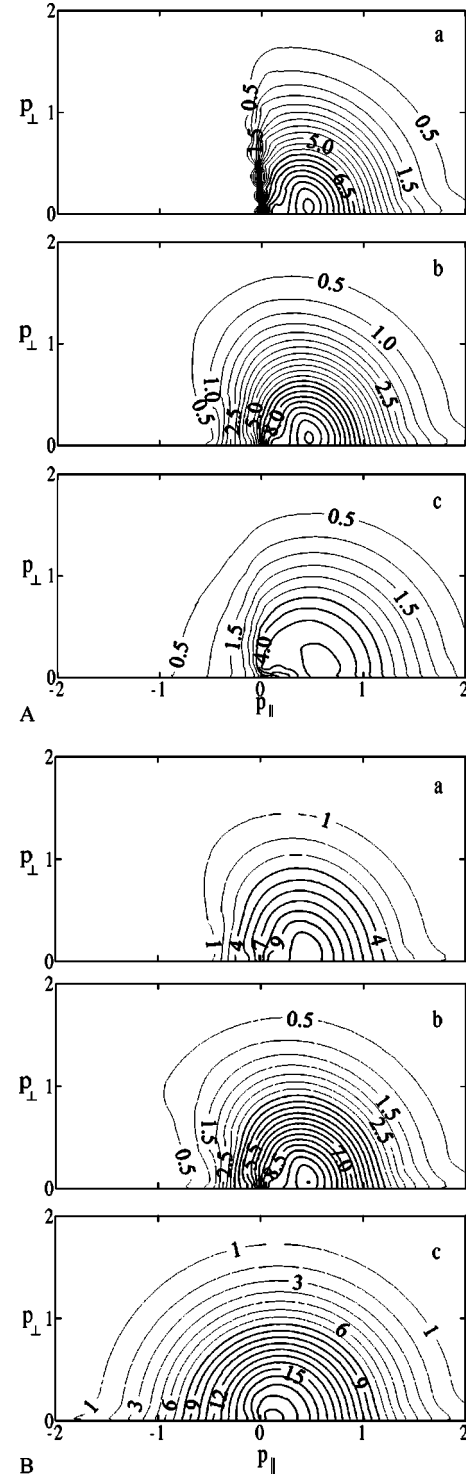


FIG. 2. Time evolution of ion distribution function $f_i(x, P_\perp, P_\parallel, t)$ in units of $10^{-2}n_0/v_i^3$ for two distances from the electrode [(A), $x=0.124$, (B), $x=0.681$] is shown for times t_i equal to (a) 0.08, (b) 0.23, (c) 0.77, $\varepsilon=2.32$.

$f_e(x, p_\perp, p_\parallel)$ decreases basically due to the influence of self-consistent electric field. Distributions obtained for electrons and ions at $x=0.681$ are rather isotropic and relatively similar. This suggests that the anisotropy in $f_e(x, p_\perp, p_\parallel)$ decays faster than the anisotropy in $f_i(x, P_\perp, P_\parallel)$.

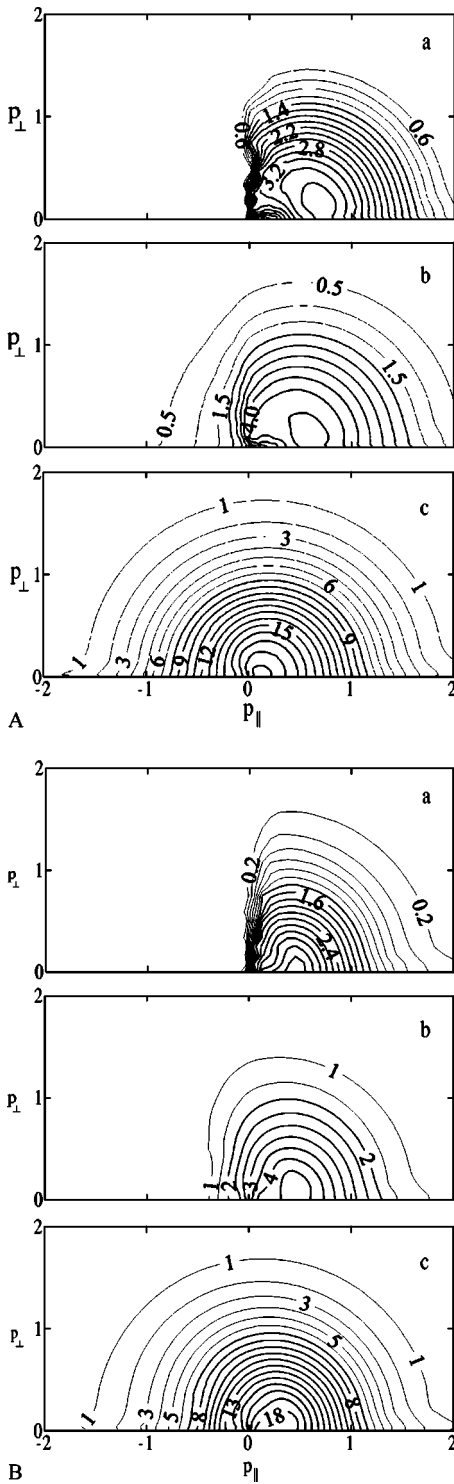


FIG. 3. Steady angular distributions of ions (A) in units of $10^{-2}n_0/v_i^3$ and electrons (B) in units of $10^{-2}n_0/v_e^3$ are shown at different distances x from the electrode: (a) 0, (b) 0.124, (c) 0.681, $\varepsilon = 2.32$.

The isotropic ion energy distribution function, $f_i(x, E)$, averaged over μ , calculated at different distances from the electrode is shown in Fig. 4(A). Solid curves show the DNS calculations, dashed curves represent the PIC-MC results, and dot-dashed curves display Maxwellian distributions. The

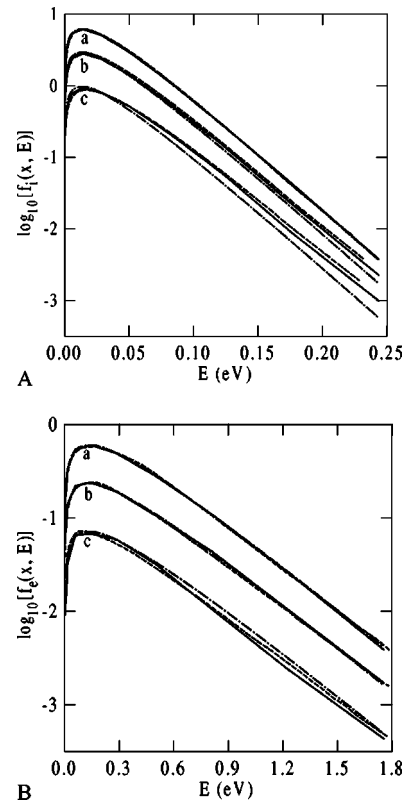


FIG. 4. Steady space- and energy-dependent distributions of ions (A) in units of n_0/v_i^3 and electrons (B) in units of n_0/v_e^3 are shown at different distances x from the electrode: (a) 23.21, (b) 7.74, (c) 0, $\varepsilon = 2.32$. Solid and dashed curves show results of the direct numerical solution and the PIC-MC simulation, respectively. The Maxwellian distribution is shown by the dot-dashed curve.

different curves $a-c$ are for decreasing distance to the electrode. The departure of $f_i(x, E)$ from a Maxwellian distribution is rather small. This suggests that ions do not experience significant heating at large ε .

The corresponding electron energy distribution function $f_e(x, E)$ is shown in Fig. 4(B). The results of the direct numerical solution shown by solid curves are in agreement with

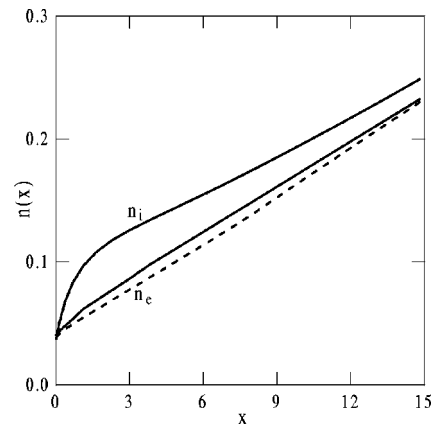


FIG. 5. Electron density $n_e(x)$ and ion density $n_i(x)$, in units of n_0 versus x for $\varepsilon = 2.32$. Solid lines show the DNS results, while the dashed line represents Eq. (29).

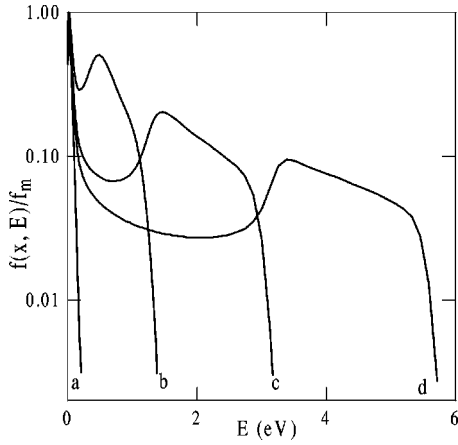


FIG. 6. Space- and energy-dependent ion distribution function $f_i(x, E)$ normalized to the maximum f_m . The positions x are equal to (b) 1.1, (c) 0.8, (d) 0.5 for $\varepsilon = 8 \times 10^{-3}$. The Maxwellian distribution is shown by curve a .

the PIC-MC simulations represented by dashed curves. We see that there is a slight departure of $f_e(x, E)$, obtained using both PIC-MC and DNS approaches, from the Maxwellian distribution for $x=0$. We checked that this departure does not play a significant role in the calculation of the electron density.

All plasma sheath models based on the solution of the hydrodynamic equations use the assumption that the electron density follows the Boltzmann relation. This relation can be obtained from the continuity equation for the electron flux neglecting frictional and inertial forces of electrons [22]. The same relation can be derived from the Boltzmann equation for the electron distribution function as follows. The electron Boltzmann equation (10) can be rewritten in the case of the steady state electron distribution function $f_e(x, \mathbf{p})$ as

$$p \frac{\partial f_e(x, \mathbf{p})}{\partial x} + \frac{1}{2} \frac{\partial \varphi(x)}{\partial x} \frac{\partial f_e(x, \mathbf{p})}{\partial p} = 0, \quad (30)$$

where we have neglected the first collisional term in Eq. (28) because $m_e/M \ll 1$ and the second collisional term owing to

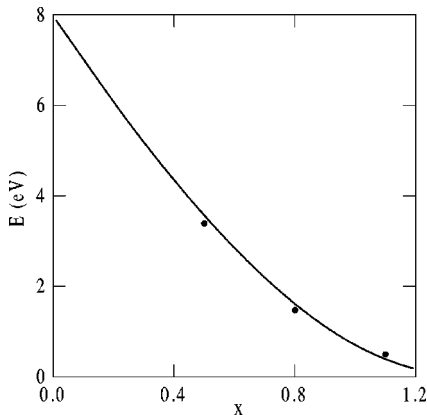
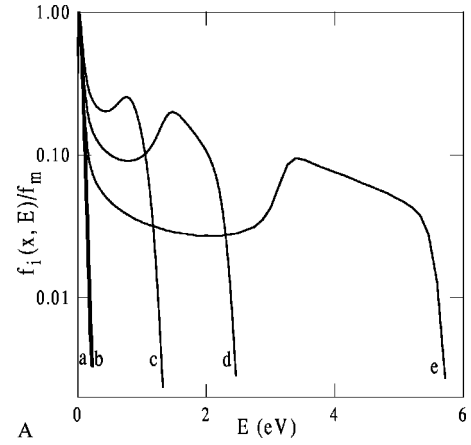
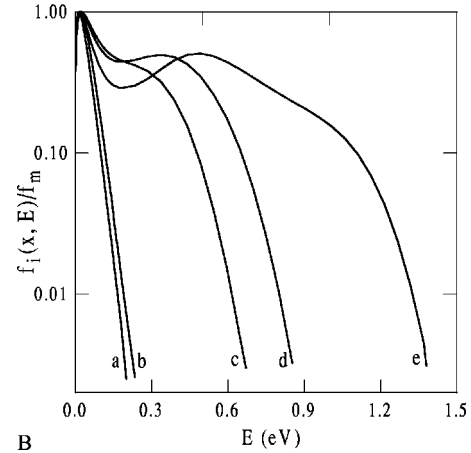


FIG. 7. The dependence of ion energy versus distance from the electrode for $\varepsilon = 8 \times 10^{-3}$. The solid line represents free-fall model, while symbols correspond to the energies of the second peaks of the curves in Fig. 6.



A



B

FIG. 8. Space- and energy-dependent ion distribution function $f_i(x, E)$ normalized to the maximum f_m for two distances to the electrode [(A), $x=0.5$, (B), $x=1.1$] is shown for ε equal to (b) 0.773, (c) 0.024, (d) 0.014, (e) 0.008. The Maxwellian source distribution is shown by curve a .

$\sigma_m/\sigma_i \ll 1$. Let us average (30) over μ and also assume that $f_e(x, p) = \int f_e(x, \mathbf{p}) d\mu$ is a local Maxwellian distribution, so that $f_e(x, p) = n_e(x) \exp(-p^2)$. Then, one can obtain using Eq. (28) the Boltzmann relation for the electron density,

$$n_e(x) = n_0 \exp[\varphi(x)], \quad (31)$$

where n_0 is the electron density at $\varphi(x)=0$.

We compare in Fig. 5 the electron density obtained using the Boltzmann relation [Eq. (29)] with the electron density obtained from the solution of Eqs. (16)–(23). Solid lines show the results of the direct solution, while dashed line represents Eq. (31). We can see a small difference between electron density, obtained using the direct numerical solution and that calculated from the Boltzmann relation. This difference arises because of the departure of electron distribution function from the local Maxwellian distribution. Additional PIC-MC calculations show that the difference between the calculated electron density and that obtained using the Boltzmann relation quickly decreases as ε drops. It suggests that at sufficiently small ε , a large number of low-energy electrons could not overcome a sheath potential barrier, and, consequently, they are repelled to the bulk plasma. It is also

important to note that the ion density does not follow the Boltzmann relation. The reason for this is that the self-consistent electric field acts differently on electron motion and ion motion. This field forces electrons out of the sheath to the bulk plasma, and, consequently, thermalizes them. Whereas, ions are dragged by the electric field from the bulk plasma to the electrode. Hence, ions are never in thermal equilibrium with the self-consistent electric field.

The distribution function of ions is shown in Fig. 6 for several distances from the electrode. The low-energy peak corresponds to the contribution from the thermal ions, whereas the high-energy peak arises because ions are heated as they move in the self-consistent electric field. The motion of high-energy ions in the sheath region is almost collisionless. This was verified by calculating the dependence of ion energy versus distance. This dependence was obtained using the ion energy conservation equation (collisionless free-fall model). The results of this calculation are shown in Fig. 7 by the solid line, and the symbols correspond to the energies at which the second peaks of curves occur in Fig. 6.

The dependence of ion energy distribution function on ε is shown in Figs. 8(A) and 8(B) for $x=0.5$ and $x=1.1$, respectively. The different curves $a-e$ are for decreasing ε .

The distribution $f_i(x,p,\varepsilon)$ calculated for $\varepsilon=0.773$ (curve b) is close to the Maxwellian distribution (curve a). This indicates that in this case ions do not experience significant heating in the sheath region. We can see two peaks in the ion energy distribution function for $\varepsilon=0.024$ (curve c). Results, obtained for smaller ε (curves d and e) show that the position of the second peak moves further from the origin as ε drops. This is because the electric field in the sheath increases with a decrease of ε . Hence, ions are more strongly heated at smaller ε . The distribution $f_i(x,p,\varepsilon)$, calculated at $x=1.1$, is shown in Fig. 8(B). In this case $f_i(x,p,\varepsilon)$ changes less dramatically with the decrease of ε . This is because ions are unable to gain significant energy at this distance from the electrode.

ACKNOWLEDGMENTS

This research was supported by a grant to B.D.S. from the Natural Sciences and Engineering Research Council of Canada. Acknowledgment is also made of the Donors of the Petroleum Research Fund administered by the American Chemical Society for support of this research (PRF No. 34689-AC6).

-
- [1] M. J. Lindenfeld and B. Shizgal, *Phys. Rev. A* **27**, 1657 (1983).
 - [2] L. Tonks and I. Langmuir, *Phys. Rev.* **34**, 876 (1929).
 - [3] S. A. Self, *Phys. Fluids* **6**, 1762 (1963).
 - [4] S. A. Self, *J. Appl. Phys.* **36**, 456 (1965).
 - [5] I. Senda, *Phys. Plasmas* **2**, 6 (1995).
 - [6] I. Senda, *Phys. Plasmas* **4**, 1308 (1997).
 - [7] H. P. van de Berg, K. U. Riemann, and G. Ecker, *Phys. Fluids B* **3**, 838 (1991).
 - [8] R. J. Procassini, C. K. Birdsall, and E. C. Morse, *Phys. Fluids B* **2**, 3191 (1990).
 - [9] J. T. Scheuer and G. A. Emmert, *Phys. Fluids* **31**, 1748 (1988).
 - [10] M. E. Riley, Sandia National Lab Report No. SAND95-00775, 1995 (unpublished).
 - [11] M. E. Riley, Sandia National Lab Report No. SAND96-1948, 1996 (unpublished).
 - [12] A. Metze, D. W. Ernie, and H. J. Oskam, *J. Appl. Phys.* **60**, 3081 (1986).
 - [13] M. A. Lieberman, *IEEE Trans. Plasma Sci.* **16**, 38 (1988).
 - [14] K.-U. Riemann, *Phys. Fluids* **24**, 2163 (1981).
 - [15] K.-U. Riemann, *J. Phys. D* **24**, 493 (1991).
 - [16] T. E. Sheridan and J. Goree, *Phys. Fluids B* **3**, 2796 (1991).
 - [17] D. J. Koch and W. N. G. Hitchon, *Phys. Fluids B* **1**, 2239 (1989).
 - [18] M. Hong and G. Emmert, *J. Vac. Sci. Technol. B* **12**, 889 (1994).
 - [19] H.-B. Valentini, *J. Phys. D* **27**, 119 (1994).
 - [20] H.-B. Valentini, E. Glauche, and D. Wolff, *Plasma Sources Sci. Technol.* **4**, 353 (1995).
 - [21] T. E. Nitschke and D. B. Graves, *IEEE Trans. Plasma Sci.* **23**, 717 (1995).
 - [22] V. A. Godyak and N. Sternberg, *IEEE Trans. Plasma Sci.* **18**, 159 (1990).
 - [23] V. A. Godyak and N. Sternberg, *Phys. Rev. A* **42**, 2299 (1990).
 - [24] M. Dalvie, S. Hamaguchi, and R. T. Farouki, *Phys. Rev. A* **46**, 1066 (1992).
 - [25] A. Gilardini, *Low Energy Electron Collisions in Gases: Swarm and Plasma Methods Applied to Their Study* (Wiley, New York, 1972).
 - [26] A. V. Vasenkov and B. D. Shizgal, *Phys. Rev. E* **63**, 016401 (2001); *Phys. Plasmas* **9**, 691 (2002).
 - [27] B. Shizgal, *J. Comp. Physiol.* **41**, 309 (1981).
 - [28] R. Blackmore and B. Shizgal, *Phys. Rev. A* **31**, 1855 (1985).
 - [29] M. Mitchner and C. H. Kruger, *Partially Ionized Gases* (Wiley, New York, 1973).
 - [30] H. Skullerud, *J. Phys. B* **6**, 728 (1973).
 - [31] S. L. Lin and J. N. Bardsley, *J. Chem. Phys.* **66**, 435 (1977).
 - [32] M. J. Brennan, *IEEE Trans. Plasma Sci.* **19**, 256 (1991).
 - [33] M. Suzuki, T. Tanigushi, and H. Tagashira, *J. Phys. D* **23**, 842 (1990).
 - [34] A. V. Phelps, *J. Phys. Chem. Ref. Data* **20**, 557 (1991).